Journal of Hazardous Materials 186 (2011) 360–366

Contents lists available at ScienceDirect

Journal of Hazardous Materials

journal homepage: www.elsevier.com/locate/jhazmat

Simultaneous photoreductive removal of copper (II) and selenium (IV) under visible light over spherical binary oxide photocatalyst

Noor Aman, T. Mishra*, J. Hait, R.K. Jana

ACC Division, National Metallurgical Laboratory, CSIR (Council of Scientific & Industrial Research), Jamshedpur-831007, India

ARTICLE INFO

Article history:
Received 9 February 2010
Received in revised form 30 October 2010
Accepted 1 November 2010
Available online 9 November 2010

Keywords:
Copper (II)
Selenium (IV)
Photoreduction
EDTA
Formic acid
Visible light

ABSTRACT

Waste water of copper mines and copper processing plant contains both copper and selenium ions with other contaminants. In this paper simultaneous photoreductive removal of copper (II) and selenium (IV) is studied for the first time using spherical binary oxide photocatalysts under visible light. All the synthesized materials are found to be mesoporous in nature with reasonably high surface area. Among a range of hole scavengers, only EDTA (ethylene diamine tetraacetic acid) and formic acid are found to be the most active for the reduction reaction. A comparative study is carried out using both the hole scavengers varying reaction time, concentration, pH etc. For a single contaminant, EDTA is found to be the best for Cu(II) reduction whereas formic acid is the best for Se(IV) reduction. In a mixed solution both EDTA and formic acid perform very well under visible light irradiation. Highest photocatalytic reduction in a mixed solution is observed at pH 3. Among all the synthesized materials, TiZr-10 performs as the best photocatalyst for both Cu(II) and Se(IV) reduction. However under UV light, Degussa P25 performs slightly better than TiZr-10. Present study shows that 100 ppm of mixed solution can be removed under visible light in 40 min of reaction using TiZr-10 as catalyst. Photodeposited material is found to be copper selenide rather than pure copper and selenium metal. This indicates that the waste water containing copper and selenium ions can be efficiently treated under visible or solar light.

1. Introduction

Presence of toxic metal ions in natural water as well as in waste water can affect the ecosystem adversely. Effluents from mining, electroplating, semiconductor industries chiefly contain copper with considerable amount of selenium [1]. Although both copper and selenium are essential as trace nutrients for living beings but become toxic if taken in higher amount. The permissible limit of copper in water is 2 mg/l whereas for selenium, it is 0.1 mg/l. The conventional methods to remove these metals from industrial waste stream are adsorption, ion-exchange, electroreduction, precipitation and membrane processes [2–4]. However, most of these techniques have their own limitations. For example, precipitation creates a significant amount of hazardous sludge which requires further treatment. In addition, complexation of metal ions with available organics often makes them inert towards waste water treatment [5]. Precipitation technologies such as hydroxide and sulfide precipitation are inhibited in presence of metal–organic complex. In this context photocatalysis is a new process having immense potential for the waste-water treatment. In recent years photocatalysis has gained importance in the area of wastewater treatment, especially in the removal of toxic metal ions e.g., Pb [6,7], Cd [8,9], Hg [10–14], Cu [15,16], Cr [17–20], Se [21–24] etc. in presence of UV and visible light. It was observed that copper removal increases particularly in presence of EDTA under UV light [25]. Selenium removal is primarily dependent on pH of the solution and the hole scavenger used [21]. EDTA itself is a contaminant found in the waste water along with other heavy metal ions. So photocatalytic removal of metal EDTA complex systems were also investigated by several authors [26–28]. However, investigation on multi metal EDTA system is rare in the literature. It is observed that in certain waste water of the copper mines and copper plants both copper and selenium are found ranging from ppb to ppm level. However to the best of our knowledge no work is reported on photocatalytic removal of Cu and Se simultaneously.

Of the various photocatalysts present, only TiO_2 is extensively used due to its non-corrosive, nontoxic, high photoactivity, high photostability and economical nature. TiO_2 in anatase form has band gap energy of 3.2 eV and thus needs light below 388 nm to be capable of producing electron–hole pairs. Since only 4% of the solar energy reaching the earth surface has wavelength below 400 nm, modified photocatalysts have to be developed for better solar applications. So for better application there is a need to develop visible light sensitive photocatalyst with high surface area

* Corresponding author. Tel.: +91 657 2345084; fax: +91 657 2345213.
E-mail address: drtmishra@yahoo.com (T. Mishra).

0304-3894/$ – see front matter © 2010 Elsevier B.V. All rights reserved.
doi:10.1016/j.jhazmat.2010.11.001

Table 1
Textural properties of the synthesized materials.

Samples	Surface area (m^2/g) at calcinations temperature of		Pore volume (cc/g) at calcinations temperature of		Average pore radius
	400 °C	500 °C	400 °C	500 °C	500 °C
Ti	103	91	0.262	0.246	59
TiZr-10	141	105	0.316	0.283	44
TiZr-20	124	96	0.291	0.252	36
TiSi-10	156	126	0.342	0.294	33
TiSi-20	163	138	0.367	0.334	23

and stable anatase phase even after calcination at higher temperature. In this context our earlier work on the formation of high surface area spherical titania based materials with increased photoreduction activity even under visible light is encouraging [29,30].

Therefore, present study is focused on the effect of different photocatalysts on visible light induced simultaneous photocatalytic removal of toxic metals like copper and selenium from acidic wastewater. Comparative effect of EDTA and formic acid on the metal reduction activity is also evaluated under visible light.

2. Materials and methods

2.1. Material synthesis

Titanium isopropoxide, zirconium butoxide and tetraethyl orthosilicate (Aldrich) were used as starting materials. Materials were synthesized according to the earlier reported method [30]. Pure titania and silica, zirconia mixed titania were prepared by controlled hydrolysis of corresponding isopropoxide in presence of surfactant (cetyltrimethylammonium bromide, CTAB) in n-propanol water mixture. Silica and zirconia (10 and 20 wt%) mixed titania samples were prepared by using calculated amount of corresponding alcoxide mixture in n-propanol so as to maintain the ratio of 10:90 and 20:80 in the binary oxides. Surfactant concentration was maintained at 2 mol% and accordingly required amount was added to the reacting mixture before hydrolysis. Hydrolysis was carried out by drop wise addition of n-propanol and water mixture from a burette under magnetic stirring condition in 30 min time period. The gel so obtained was maintained in the same stirring condition for another 4 h. Subsequently the gel was filtered and washed with distilled water several times, dried at 100 °C, calcined at 500 °C for 4 h and kept for further use. Silica mixed titania and zirconia mixed titania are denoted as TiSi and TiZr, respectively. Number after the sample indicates the weight percentage of silica or zirconia mixed with titania.

2.2. Material characterization

BET surface area and pore size distribution was determined by N_2 adsorption desorption method at liquid nitrogen temperature using Nova 4000e (Quantachrome, USA). Prior to adsorption desorption measurements, the samples were degassed at 473 K at 10^{-3} Torr for 5 h.

SEM micrographs of powdered samples were recorded on scanning electron microscope (JEOL 840A, Japan) after gold coating.

FT-IR spectra of different samples were recorded with Nicolet 750 FT-IR spectrometer using KBr palate at room temperature in the range of 400–4000 cm^{-1} with scanning rate of 4 cm^{-1}/min.

XRD patterns of all the synthesized samples calcined at different temperatures were recorded on a Siemens (model: D-500) semiautomatic diffractometer using Cu-Kα radiation source and Ni filter in the range of 10–90°.

X-ray photoelectron spectra (XPS) were recoded by UHV analysis system (SPECS, Germany) with an Al-Kα monochromatized X-ray source (E = 1486.6 eV). The instrument was operated at a pressure 6×10^{-9} Torr in the analysis chamber. The binding energies were collected with a reference to the maximum intensity of the C 1s (285.0 eV).

2.3. Photocatalytic activity

Prepared materials, after calcination at different temperatures were used as photocatalyst for the reductive removal of selenium and copper ions at different pH. Stock solution of selenium and copper was prepared by dissolving required amount of sodium selenite and copper sulphate salts in double distilled water. Photocatalytic activity is also dependent on the type of reactor and the light intensity [31]. All the photocatalytic experiments were carried out in a 200 ml capacity three necked glass reactor of 25 cm length and 4.9 cm internal diameter (Fig-S1 of Supplementary information). Centrally fitted 125 W high pressure mercury lamp with most intense peak at 546 nm was used as visible light source (Fig-S2 of Supplementary information). It was almost same for all the photocatalysts. Constant reaction temperature was maintained through water circulation in the outer jacket of the lamp, external and internal diameter being 4.2 and 2.8 cm, respectively. All the experiments were performed in presence of air at atmospheric pressure and constant magnetic stirring condition. Initial concentration of metal ions in mixed solution was maintained at 100 ppm having Cu(II) and Se(IV) in 1:1 molar ratio in each experiment. For all the experiments 0.1 g of photocatalyst was dispersed in 100 ml of solution. Solution pH was adjusted as per requirement by the addition of dilute HCl and NaOH. After reaction, metal deposited solid catalyst was separated by filtration or centrifuge. Metal ion concentration in the solution after and before reaction was estimated by Analyst AAS 400 (Perkin Elmer).

3. Result and discussion

All the synthesized catalysts show mostly anatase phase after calcinations at 500 °C, with mostly uniform spherical shapes having average diameter in the range of 0.8–1 μm [30]. Materials show type IV isotherm with hysteresis loops (Fig-S3 of Supplementary information), indicating their mesoporous nature. The pore size distribution was calculated from desorption branch of nitrogen isotherm by BJH method and presented in Fig-S4 of Supplementary information. Textural properties are tabulated in Table 1, which shows that the average pore diameter decreases on subsequent addition of silica and zirconia to the titania. This indicates that the contribution of smaller pores increases in case of binary oxide materials in comparison to the pure titania. Increased pore volume and BET surface area in case of silica and zirconia mixed titania is partially explained by the presence of micropores as evident from isotherm. However, pore volume and BET surface area further increase due to the increasing silica content from 10 wt% to 20 wt%.

According to XPS measurements, $Zr3d_{5/2}$ peak of TiZr-10 is composed of two signals at binding energies of 182.03 and 181.3 eV (Fig. 1). When these values are compared with pure ZrO_2, the binding energy at 182.03 eV and 181.3 eV is attributed to $Zr3d_{5/2}$ in pure

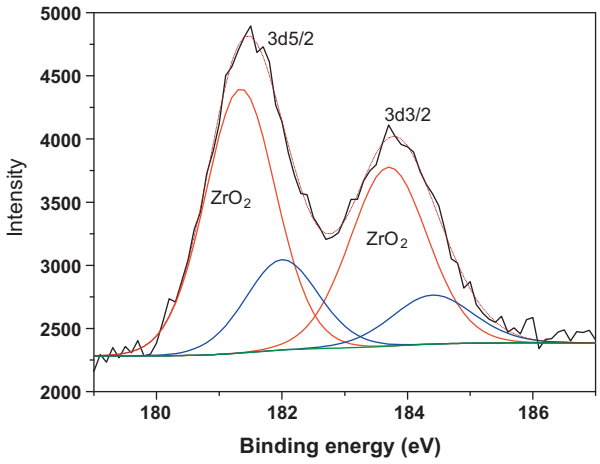

Fig. 1. Zr3d XPS spectra of TiZr-10 material.

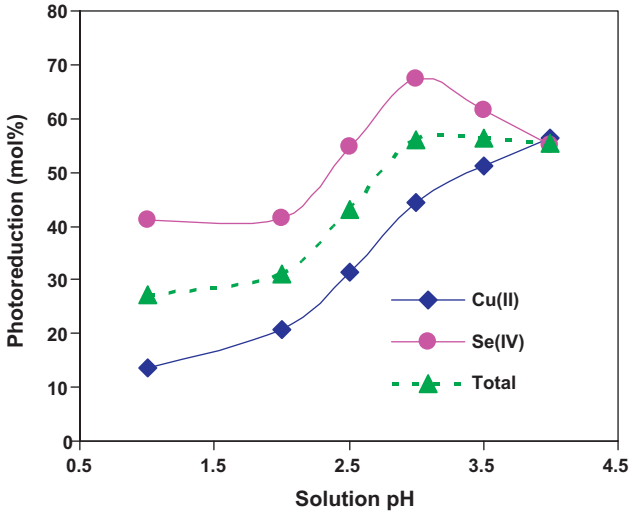

Fig. 2. Effect of pH on the simultaneous photoreduction of Cu (II) and Se (IV) within 20 min of the reaction using 400 ppm formic acid as hole scavenger over TiZr10.

ZrO_2 and $Zr3d_{5/2}$ of Zr doped TiO_2, respectively. Similarly $Zr3d_{3/2}$ can be deconvoluted to two peaks as shown in Fig. 1. This confirms the partial zirconium doping in TiO_2 lattice. Rest of the zirconium mostly remains distributed at the grain boundaries thus inhibiting the crystallite growth and phase transformation.

3.1. Effect of hole scavenger

In this study, effect of eight hole scavengers like methanol, propanol, triethanolamine, formic acid, oxalic acid, succinic acid, citric acid and EDTA disodium salt were studied. Their effect on the simultaneous photoreduction of Cu(II) and Se(IV) are summarized in Table 2. Total photoreduction increases in the order of EDTA > formic acid > oxalic acid > triethanolamine > propanol > methanol > succinic acid. Interestingly for the mixed solution, EDTA proves to be a good hole scavenger like formic acid. In particular, selenium reduction increases in a mixed solution when EDTA is used as hole scavenger. From the adsorption data it is observed that comparative Se(IV) adsorption in presence of EDTA increases from 4% to 7% due to the presence of Cu(II). In a mixed solution at pH 3, nearly equal amount of copper and selenium were adsorbed in dark experiment. Hence EDTA is acting like a strong hole scavenger which helps in direct transfer of electron to the valence band of the photocatalyst. It is proposed that electrons from EDTA are directly filled to the valence band, thereby inhibiting the e^-–h^+ recombination and leaving more conduction band electrons available for reduction of metal ions [32,33]. Similar trend is also observed for different hole scavengers in case of Cr(VI) reduction [33]. However, in case of alcohols, amines and acids (except formic acid), holes are filled only through the formation of hydroxyl radicals. These radicals evidently decompose organics. This indirect route of organic decomposition of alcohols, amines and carboxylic acids (except formic acid) make them less active hole scavenger. Undoubtedly hole scavenger has a definite role in the photoreduction activity. There is a good correlation between the degradation rates and chemical structure of the organics. It is reported that the rate of photodegradation of organics can be influenced by different electron acceptors [33]. Therefore, choice of hole scavenger is quite important. Based on the above results we have studied in detail the effect of EDTA and formic acid only as hole scavenger.

3.2. Effect of pH

Photocatalytic reduction of any metal ion is considerably influenced by solution pH. Position of both conduction band and valence band is pH dependent. The potential of both conduction band and valence band shift to cathodic potential by 59 mV per pH unit.

$$E_{cb} = -0.3–0.059\text{pH}(\text{at}25\,^{\circ}\text{C}, \text{pH}0) \quad (1)$$

$$E_{vb} = 2.9–0.059\text{pH}(\text{at}25\,^{\circ}\text{C}, \text{pH}0) \quad (2)$$

Photoreduction of Cu(II) and Se(IV) from mixed solution was investigated in a range of pH using formic acid as hole scavenger to understand the role of solution pH on the photoreduction activity (Fig. 2). It is observed that the selenium reduction increases with increasing the pH up to 3 and then decreases sharply. However copper reduction increases with the increasing pH. Optimum pH for simultaneous removal of Cu(II) and Se(IV) is found to be 3. On decreasing the pH below 3, total photoreduction also decreases sharply as shown in Fig. 2. This decrease in photoreduction can be attributed to low ionization of formic acid at higher acidic condition which minimizes the formic acid adsorption on the catalyst surface. Hole scavenger (formic acid) adsorption also regulates the photoreduction of selenium [21]. Similar observation on the effect of pH was also reported earlier [21]. In case of copper reduction, there is gradual leaching of deposited copper metal at low pH which leads to low copper deposition.

3.3. Photocatalytic activity of copper and selenium

It is observed that copper (II) and selenium (IV) individually reduced to metallic copper and elemental red selenium under photocatalytic reaction and deposited on the catalyst surface. Hence accordingly colour of the catalyst changes after reaction. Fig. 3 shows the photocatalytic reduction of Cu(II) in presence of formic

Table 2
Effect of different hole scavengers on the simultaneous photoreduction of Cu (II) and Se(IV) after 25 min of reaction.

Hole scavenger	Formic acid	EDTA	Citric acid	Oxalic acid	Triethanol amine	Propanol	Methanol	Succinic acid
Cu (II)	71	81	61	59	62	60	46	31
Se(IV)	83	90	68	81	66	63	59	40

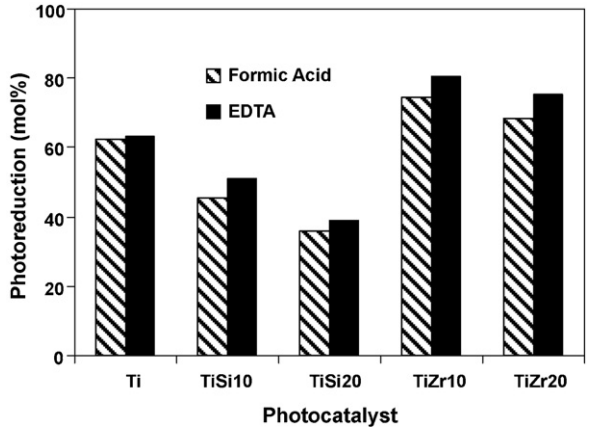

Fig. 3. Photoreduction of 50 ppm Cu (II) over the synthesized catalysts within 22 min of reaction in presence of 200 ppm of hole scavenger at pH 3.

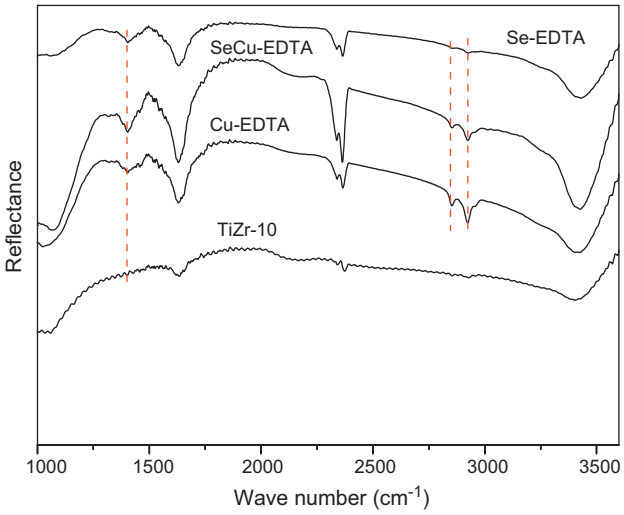

Fig. 5. FTIR spectra of TiZr-10 after dark adsorption of EDTA in presence of Se (IV) and Cu (II) after 30 min of reaction using formic acid as hole scavenger over TiZr-10 catalyst.

acid and EDTA. EDTA behaves as better hole scavenger than formic acid for copper reduction. Enhanced photocatalytic reduction in presence of EDTA may be due to strong adsorption of metal–EDTA complex on the catalyst surface. Moreover enhanced hole scavenging capacity of the intermediates formed during the oxidative degradation of EDTA [27] helps to increase the photocatalytic activity. Copper is completely reduced to Cu (0) within 22 min of reaction over TiZr-10 catalyst under visible light. However, TiSi-10 and TiSi-20 show lesser activity than other photocatalysts used despite having higher surface area. Effect of formic acid and EDTA were also studied on the photoreduction of Se(IV), as shown in Fig. 4. In contrast to Cu(II) photoreduction, formic acid is found to be a better hole scavenger than EDTA for Se(IV) photoreduction. Selenium (IV) photoreduction in presence of EDTA decreases to nearly 50% in comparison to the formic acid. Complete photoreduction of Se(IV) to red Se(0) is achieved in 15 and 35 min of the reaction in presence of formic acid and EDTA, respectively. It is well understood that both, hole scavengers and the selenite are anionic species and hence compete each other for adsorption on the catalyst surface during reaction. Mostly size of the anions and their attachment on the catalyst surface play an important role in the photoreduction activity. To understand the adsorption behavior of EDTA we recorded the FTIR spectra of titania after 20 min dark adsorption of EDTA in presence of Se(IV) and Cu(II) were recorded and presented in Fig. 5. Peaks at 1406, 2854 and 2926 cm^{-1} indicate the presence of EDTA on the titania surface. It is well marked that EDTA adsorption is low in case of only Se(IV) in comparison to only Cu(II) and Cu(II) + Se(IV) in solution. Due to the smaller size, selenite adsorption increases thereby decreasing the EDTA adsorption on the catalyst surface which subsequently decreases the photoreduction activity. However similar effect is not noticed in case of copper reduction as copper is present as cation. In case of selenite reduction, TiZr-10 again performs as the best catalyst, whereas minimum reduction is observed over TiSi-10 and TiSi-20 catalysts. This difference in the photocatalytic activity may be due to the presence of more surface active sites in TiZr-10, resulting in better photoreduction activity. Moreover visible light absorption is minimum with the silica mixed samples in comparison to TiZr materials [30] and hence the photocatalytic activity under visible light decreases. In case of TiZr materials partial zirconium doping in the titania helps in the increase of photocatalytic activity under visible light. Besides, presence of the zirconium oxide also increases the surface acidity of the material thus facilitating the photocatalytic activity. So it can be concluded that only surface area is not an important parameter for increased photocatalytic activity.

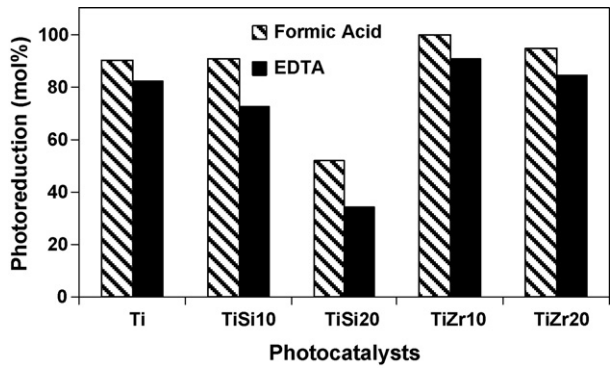

Fig. 4. Photoreduction of 50 ppm Se (IV) over the synthesized catalysts within 22 min of reaction in presence of 200 ppm of hole scavenger at pH 3.

3.4. Photo reduction from mixed solution

With TiO_2 alone as photocatalyst low photoreduction was noticed and this may be due to more favorable e^-–h^+ recombination. However, on addition of suitable organics, photoreduction of both Cu(II) and Se(IV) increases many fold by virtue of scavenging of holes by the organics in their oxidative degradation.

Based on the preliminary results of different hole scavengers we have studied the effect of formic acid and EDTA on the photoreduction of selenium and copper in a mixed solution having 50 ppm of Cu(II) and 50 ppm of Se(IV) in detail. Initially formic acid is found to be slightly better hole scavenger for both copper and selenium reduction in comparison to that of EDTA (Fig. 6). This is mostly due to the small size of the formate anion in comparison to the EDTA. We also studied the photocatalytic activity varying the hole scavenger amount. On increasing the hole scavenger (formic acid and EDTA) concentration from 200 ppm to 400 ppm, reduction of both the ions increases appreciably. Optimum requirement of both formic acid and EDTA is 400 ppm for 100 ppm of mixed solution as further increase of formic acid and EDTA has negligible effect on the photoreduction activity (Fig-S5, Supplementary information). Quite surprisingly, it was observed that in contrary to the individual Se(IV) reduction, EDTA addition increases the Se(IV) photoreduction in mixed solution (Table 3). We also tried to investigate the effect of different catalysts on Cu to Se removal ratio. It is well observed in the Table 3 that copper to selenium removal ratio is more when formate is used as hole scavenger in compari-

Table 3
Photocatalytic reduction of Cu(II) and Se(IV) in mixed solution after 15 min of reaction over synthesized catalysts in presence of formic acid and EDTA as hole scavenger.

Photocatalyst used	Photoreduction in presence of formic acid (mol%)			Photoreduction in presence of EDTA (mol%)		
	Cu(II)	Se(IV)	Cu/Se	Cu(II)	Se(IV)	Cu/Se
Ti	56	66	0.848	55	68	0.809
TiSi-10	55	65	0.846	52	66	0.788
TiSi-20	52	62	0.839	51	64	0.797
TiZr-10	62	76	0.829	65	81	0.802
TiZr-20	58	68	0.853	60	76	0.789

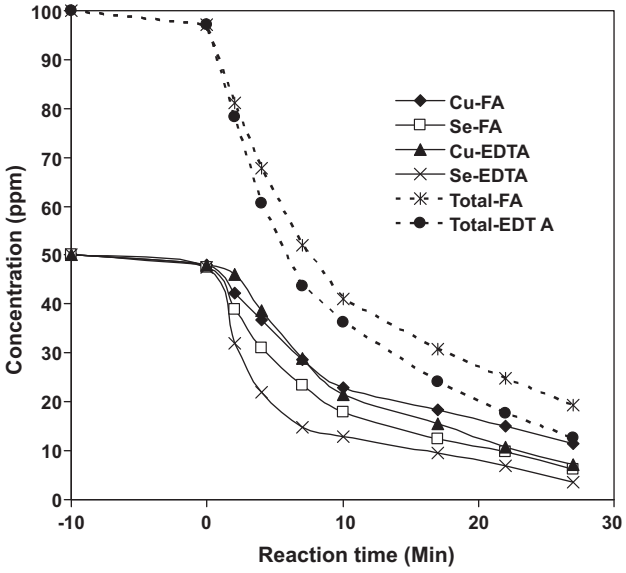

Fig. 6. Effect of time on the photoreduction of Cu (II) and Se (IV) from a mixed solution at pH 3 over TiZr-10 using 400 ppm formic acid/EDTA as hole scavenger.

son to EDTA. This ratio more or less remains same for a particular hole scavenger even when catalysts are varied. Comparative photoreduction study of both copper and selenium over TiZr-10 and commercial Degussa P25 catalyst is presented in Figs. 7 and 8. It is observed that under visible light irradiation synthesized material TiZr-10 performs far better than the Degussa P25. However, under UV light commercial Degussa P25 performs slightly better than TiZr-10. Increased visible light activity also justifies the non-metal doping or oxygen vacancy creation in the material during

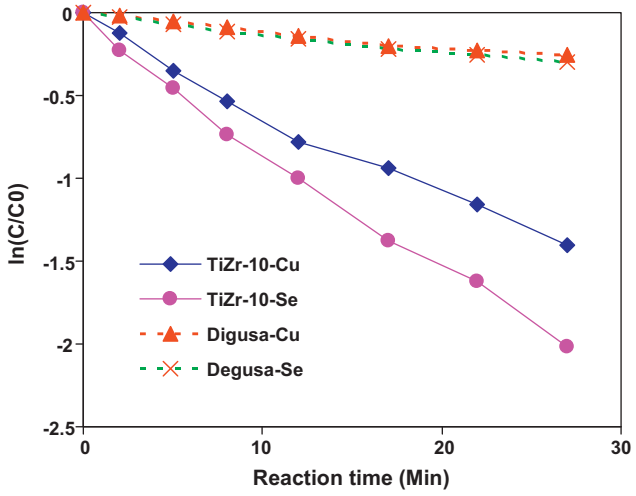

Fig. 7. Plot of $\ln(C/C_0)$ with time for simultaneous reduction of selenium and copper under visible light using TiZr-10 or Degussa P25 and 400 ppm formic acid as hole scavenger.

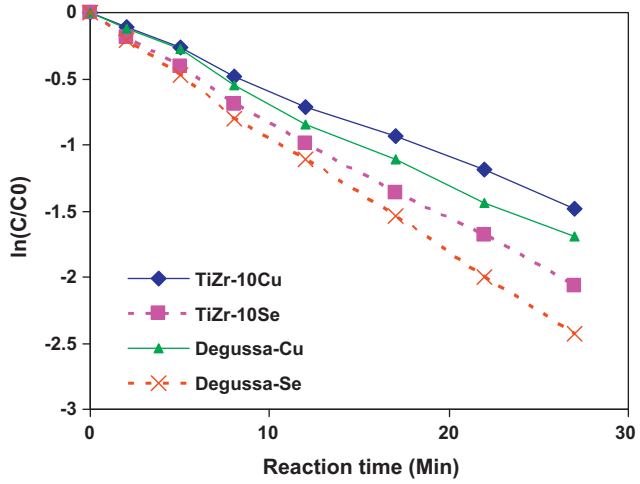

Fig. 8. Plot of $\ln(C/C_0)$ with time for simultaneous reduction of selenium and copper under UV light using TiZr-10 and Degussa P25 in presence of 400 ppm formic acid.

the synthesis. In particular, increased visible light performance of zirconium doped titania has also been reported earlier [30,34]. It is understood that any doping which creates bulk or surface sites above the valence band edge of TiO_2 results in decreased UV-light photocatalytic activity compared to undoped titania [35]. This explains the slight decrease in the activity under UV light. Following equation is applied to calculate the quantum yield (η) of the photocatalytic reaction.

$$\eta = \frac{\text{Amount (mol) of the reactant consumed or product formed}}{\text{Amount (einstein) of photons absorbed during reaction period}}$$

Fig. 9 shows the quantum yield of all the photocatalysts for simultaneous reduction of Cu(II) and Se(IV) in presence of 400 ppm formic acid. Fig. 9 also shows that the TiZr-10 has the best quantum yield under visible light. The present result confirms that the

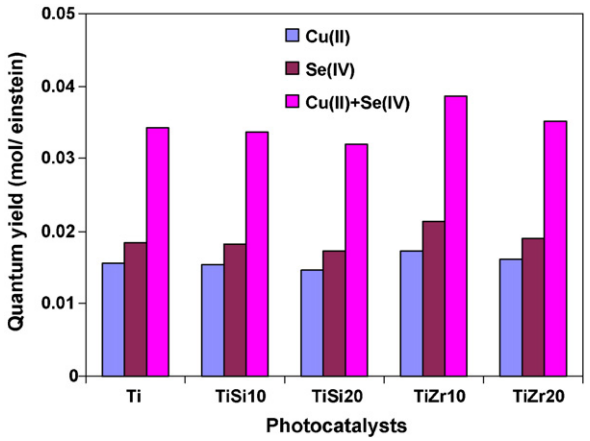

Fig. 9. Quantum yield for Cu (II) and Se (IV) mixed solution reduction on different photocatalysts.

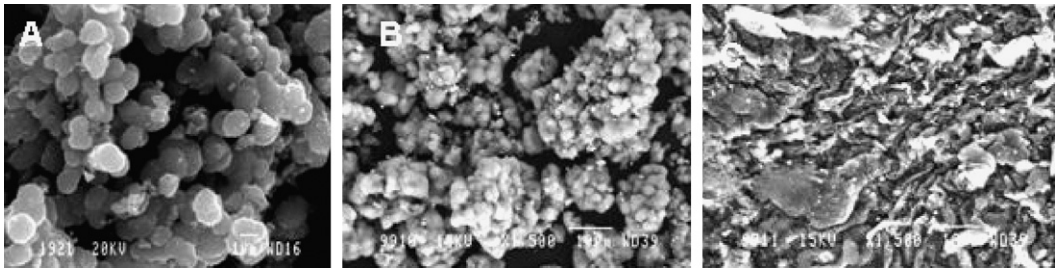

Fig. 10. SEM images of the photocatalyst (a) before and after (b) 15 and (c) 35 min of reaction.

synthesized material can be utilized as a photocatalyst both under visible and UV light. Complete photoreduction of 100 ppm mixed solution is observed over TiZr-10 in 40 min of reaction at pH 3. However, with higher contaminant amount (>100 ppm) it is difficult to remove all the metal ions completely in a single batch. This inactivation of the catalyst is mostly due to the deposition of metals on the catalyst surfaces. The metal removal capacity of the catalyst is also dependent on the surface area of the material. Similar catalyst inactivation is also observed in case of Cr(VI) reduction [36].

It is observed that Se(IV) photoreduction rate is more than that of Cu(II) reduction. This is due to the more positive reduction potential of Se(IV) ($Se^{4+}/Se = 0.74$ V) than Cu(II) ($Cu^{2+}/Cu = 0.34$ V). Photoreduction is possible when the reduction potential of the reactant is more positive than the conduction band potential of the catalyst (−0.3 V). As reduction potential of both Cu(II) and Se(IV) both are positive so the simultaneous reduction of Cu(II) along with Se(IV) is observed. Irrespective of different reduction potentials simultaneous reduction of Cu(II) and Se(IV) is observed in the present study. SEM images show the catalyst (TiZr-10) before reaction, after 15 min and 35 min of the reactions (Fig. 10). This clearly indicates that deposition of the metal gradually increases with the reaction time and ultimately completely covers the catalyst surface. Complete coverage of the catalyst surface deactivates the catalyst. However, catalyst can be reactivated by proper removal of deposited materials through washing. Deactivated catalyst can be reused after washing at least for 5 times, with only 4% decrease in activity. So the present photocatalytic process can be used under a batch process for the removal of copper and selenium under solar light.

XRD of the photocatalyst after reaction indicates the formation of copper selenide instead of pure copper and selenium metal (Fig-S6, Supplementary information). Presence of two sharp peaks at 46.4 and 49.44 two theta values are due to respective 110 and 108 faces of CuSe. Since the reaction is occurring at molecular level, therefore following mechanism is proposed for the CuSe formation.

$$Cu(II) + 2e^- \rightarrow Cu \quad (3)$$

$$Se(IV) + 4e^- \rightarrow Se \quad (4)$$

$$Cu + Se \rightarrow CuSe \quad (5)$$

This indicates that in a multicomponent systems one can deposit different alloys on the oxide surface through photocatalytic process which is quite interesting for material development.

4. Conclusion

Simultaneous photoreductive removal of copper (II) and selenium (IV) was studied using spherical binary oxide photocatalysts under visible light from a mixed aqueous solution. In contrast to the Cu(II) photoreduction, formic acid is found to be better hole scavenger than EDTA for Se(IV) in a single contaminant reaction. Optimum requirement of both formic acid and EDTA is 400 ppm for 100 ppm of mixed solution as further increase has negligible effect on the photoreduction activity. It is also observed that in contrast to the individual Se(IV) reduction, EDTA addition increases the Se(IV) photoreduction in mixed solution. It is well observed that under visible light irradiation synthesized TiZr-10 performs far better than the Degussa P25. However, under UV light Degussa P25 performs slightly better than TiZr-10. 100 ppm of mixed solution can be completely photoreduced over TiZr-10 in 40 min of reaction. Catalyst can be reused at least for five times with marginal change in the activity. Above study indicates that using a batch process, synthesized catalyst TiZr-10 can be used for the treatment of wastewater containing copper and selenium even under solar light. XRD of the photocatalyst after reaction indicates the formation of copper selenide instead of pure copper and selenium metal. This indicates that in a multicomponent systems one can deposit different alloys on the oxide surface through photocatalytic process which is quite interesting for material development.

Acknowledgments

Authors are thankful to Dr. S. Srikanth, Director, NML for his encouragement and permission to publish the work. One of the authors Noor Aman is thankful to the CSIR for providing senior research fellowship.

Appendix A. Supplementary data

Supplementary data associated with this article can be found, in the online version, at doi:10.1016/j.jhazmat.2010.11.001.

References

[1] Y.F. Zhao, G.A. Irons, The kinetics of selenium removal from molten copper by powder injection, Metall. Mater. Trans. B 28 (1997) 1039–1051.
[2] N.L. Nemerow, Liquid Waste of Industry: Theories, Practices and Treatment, Addison-Wesley, Reading, MA, 1971.
[3] F.W. Pontius, Water Quality and Treatment: A Handbook of Community Water Supplies, fourth ed., Mc-Graw Hill, New York, 1990.
[4] R.W. Peters, Y. Ku, D. Bhattacharyya, Evaluation of recent treatment techniques for removal of heavy metals from industrial wastewaters, in: R.W. Peters, B.M. Kim (Eds.), Separation of Heavy Metals and Trace Contaminates, AIChE Symposium Series, Vol. 81, 1985, pp. 165–203.
[5] J.M. Cleveland, T.F. Rees, Characterization of plutonium in maxey flats radioactive trench leachates, Science 212 (1981) 1506–1509.
[6] K. Tennakone, K.G.U. Wijayantha, Heavy-metal extraction from aqueous medium with an immobilized TiO_2 photocatalyst and a solid sacrificial agent, J. Photochem. Photobiol. A: Chem. 113 (1998) 89–92.
[7] L. Murruni, G. Leyva, M.I. Litter, Photocatalytic removal of Pb(II) over TiO_2 and Pt-TiO_2 powders, Catal. Today 129 (2007) 127–135.
[8] C.R. Chenthamarakshan, K. Rajeshwar, Photocatalytic reduction of divalent zinc and cadmium ions in aqueous TiO_2 suspensions: an interfacial induced adsorption-reduction pathway mediated by formate ions, Electrochem. Commun. 2 (2000) 527–530.
[9] I.A. Ruvarac-Bugarcic, Z.V. Saponjic, S. Zec, T. Rajh, J.M. Nedeljkovic, Photocatalytic reduction of cadmium on TiO_2 nanoparticles modified with amino acid, Chem. Phys. Lett. 407 (2005) 110–113.
[10] E. Gkika, A. Troupis, A. Hiskia, E. Papaconstantinou, Photocatalytic reduction and recovery of mercury by polyoxometalates, Environ. Sci. Technol. 39 (2005) 4242–4248.

[11] F. Zhang, J.O. Nriagu, H. Itoh, Photocatalytic removal and recovery of mercury from water using TiO_2-modified sewage sludge carbon, J. Photochem. Photobiol. A: Chem. 167 (2004) 223–228.
[12] L.B. Khalil, M.W. Rophael, W.E. Mourad, The removal of the toxic Hg(II) salts from water by photocatalysis, Appl. Catal. B: Environ. 36 (2002) 125–130.
[13] X. Wang, S.O. Pehkonen, A.K. Ray, Photocatalytic reduction of Hg(II) on two commercial TiO_2 catalysts, Electrochim. Acta 49 (2004) 1435–1444.
[14] S.G. Botta, D.J. Rodriguez, A.G. Leyva, M.I. Litter, Features of the transformation of Hg(II) by heterogeneous photocatalysis over TiO_2, Catal. Today 76 (2002) 247–258.
[15] T. Kanki, H. Yoneda, N. Sano, A. Toyoda, C. Nagai, Photocatalytic reduction and deposition of metallic ions in aqueous phase, Chem. Eng. J. 97 (2004) 77–81.
[16] N.S. Foster, R.D. Noble, C.A. Kova, Reversible photoreductive deposition and oxidative dissolution of copper ions in titanium dioxide aqueous suspensions, Environ. Sci. Technol. 27 (1993) 350–356.
[17] P. Mohapatra, T. Mishra, K.M. Parida, Effect of microemulsion composition on textural and photocatalytic activity of titania nanomaterial, Appl. Catal. A: Gen. 310 (2006) 183–189.
[18] L.B. Khalil, W.E. Mourad, M.W. Rophael, Photocatalytic reduction of environmental pollutant Cr(VI) over some semiconductors under UV/visible light illumination, Appl. Catal. B: Environ. 17 (1998) 267–273.
[19] C.R. Chenthamarakshan, K. Rajeshwar, Heterogeneous photocatalytic reduction of Cr(VI) in UV-irradiated titania suspensions: effect of protons, ammonium ions and other interfacial aspects, Langmuir 16 (2000) 2715–2721.
[20] L. Wang, N. Wang, L. Zhu, H. Yu, H. Tang, Photocatalytic reduction of Cr(VI) over different TiO_2 photocatalysts and the effects of dissolved organic species, J. Hazard. Mater. 152 (2008) 93–99.
[21] T.T.Y. Tan, D. Beydoun, R. Amal, Photocatalytic reduction of Se(VI) in aqueous solutions in UV/TiO_2 system: importance of optimum ratio of reactants on TiO_2 surface, J. Mol. Catal. A: Chem. 202 (2003) 73–85.
[22] T.T.Y. Tan, D. Beydoun, R. Amal, Photocatalytic reduction of Se(VI) in aqueous solutions in UV/TiO_2 system: kinetic modeling and reaction mechanism, J. Phys. Chem. B 107 (2003) 4296–4303.
[23] T. Tan, D. Beydoun, R. Amal, Effects of organic hole scavengers on the photocatalytic reduction of selenium anions, J. Photochem. Photobiol. A: Chem. 159 (2003) 273–280.
[24] V.N.H. Nguyen, R. Amal, D. Beydoun, Photocatalytic reduction of selenium ions using different TiO_2 photocatalysts, Chem. Eng. Sci. 60 (2005) 5759–5769.
[25] N.S. Foster, A.N. Lancaster, D.Noble Richard, C.A. Koval, Effect of organics on the photodeposition of copper in titanium dioxide aqueous suspensions, Ind. Eng. Chem. Res. 34 (1995) 3865–3871.
[26] A.P. Davis, D.L. Green, Photocatalytic oxidation of cadmium-EDTA with titanium dioxide, Environ. Sci. Technol. 33 (1999) 609–617.
[27] J.K. Yang, A.P. Davis, Photocatalytic oxidation of Cu(II)-EDTA with illuminated TiO_2: mechanisms, Environ. Sci. Technol. 34 (2000) 3796–3801.
[28] T.H. Madden, A. Datye, M. Fulton, M.R. Prairie, S. Majumdar, B. Stange, Oxidation of metal-EDTA complexes by TiO_2 photocatalysis, Environ. Sci. Technol. 31 (1997) 3475–3481.
[29] T. Mishra, J. Hait, Noor Aman, R.K. Jana, S. Chakraborty, Effect of UV and visible light on photocatalytic reduction of lead and cadmium over titania based binary oxide, J. Colloid Interface Sci. 316 (2007) 80–84.
[30] T. Mishra, J. Hait, Noor Aman, M. Gunjan, B Mahato, R.K. Jana, Surfactant mediated synthesis of spherical binary oxides photocatalyst with enhanced activity in visible light, J. Colloid Interface Sci. 327 (2008) 377–383.
[31] G. Li Puma, V. Puddu, H.K. Tsang, A. Gora, B. Toepfer, Photocatalytic oxidation of multicomponent mixtures of estrogens (estrone (E1) 17β-estradiol (E2), 17α -ethynylestradiol (EE2) and estriol(E3)) under UVA and UVC radiation: photon absorption, quantum yields and rate constants independent of photon absorption, Appl. Catal. B: Environ. 99 (2010) 388–397.
[32] M.R. Prairie, L.R. Evans, B.M. Stange, S.L. Martinez, An investigation of titanium dioxide photocatalysis for the treatment of water contaminated with metals and organic chemicals, Environ. Sci. Technol. 27 (1993) 1776–1782.
[33] N. Wang, L. Zhu, Y. Huang, Y. She, Y. Yu, H. Tang, Drastically enhanced visible light photocatalytic degradation of colorless aromatic pollutants over TiO_2 via a charge-transfer complex path: a correlation between chemical structure and degradation rate of the pollutants, J. Catal. 266 (2009) 199–206.
[34] J. Lukac, M. Klementova, P. Bezdicka, S. Bakardjieva, J. Subrt, L. Szatmary, Z. Bastl, J. Jirkovsky, Influence of Zr as TiO_2 doping ion on photocatalytic degradation of 4-chlorophenol, Appl. Catal. B: Environ. 74 (2007) 83–91.
[35] V. Pore, M. Ritala, M. Leskela, S. Areva, M. Jarn, J. Jarnstrom, H_2S modified atomic layer deposition process for photocatalytic TiO_2 thin films, J. Mater. Chem. 17 (2007) 1361–1371.
[36] N. Wang, Y. Xu, L. Zhu, X. Shen, H. Tang, Reconsideration to the deactivation of TiO_2 catalyst during simultaneous photocatalytic reduction of Cr(VI) and oxidation of salicylic acid, J. Photochem. Photobiol. A: Chem. 201 (2009) 121–127.